NUCL SCI TECH (2018) 29:30
https://doi.org/10.1007/s41365-018-0359-3

Sorption of uranium(VI) from aqueous solutions by DEEA organo-volcanic: isotherms, kinetic and thermodynamic studies

Ümit H. Kaynar[1] · Ümran Hiçsönmez[2] · Sermin Çam Kaynar[3] · Süleyman Koçak[2]

Received: 4 February 2017 / Revised: 20 April 2017 / Accepted: 29 April 2017 / Published online: 13 February 2018

Abstract The sorption of the uranium(VI) ions from aqueous solutions by diethylethanolammonium organo-volcanics (Kula-TURKEY) was investigated under different experimental conditions. DEEA was used to modify the surface of basaltic volcanics. The characteristic of basaltic volcanic was analyzed by XRF, SEM–EDS, FTIR, and XRD. The BET surface areas of unmodified volcanics and DEEA-modified volcanics were found as 2.265 and 3.689 m^2/g, respectively. The volcanic samples were treated by using different concentrations of DEEA. The adsorption of U(VI) on natural and modified volcanics was examined as a function of the contact time, initial pH of the solution, initial U(VI) concentration, and temperature. Langmuir, Freundlich, and D–R adsorption isotherms were used to describe the adsorption. While examining the adsorption percentage and distribution coefficient, these values for unmodified volcanics were found to be 25% ± 0.76 and 10.08 mL/g, while the values for the DEEA-modified volcanics were 88% ± 1.04 and 220 mL/g, respectively. The pseudo-first-order and pseudo-second-order kinetic models were used to describe the kinetic data. In this study, it can be seen that the adsorption process is suitable for the pseudo-second-order kinetic model. Various thermodynamic parameters ($\Delta G°$, $\Delta H°$, and $\Delta S°$) were calculated with the thermodynamic distribution coefficients obtained at different temperatures. The sorption process was a chemical adsorption process. The results indicated that the processes are spontaneous and endothermic.

Keywords DEEA · Kula volcanics · Uranium · Adsorption · Isotherm

1 Introduction

Thorium and uranium mining, nuclear fuel cycle processes, nuclear power plant decontamination of nuclear facilities, and institutional uses of radioisotopes such as by agriculture, industry, research reactors and medicine are among the main sources of radioactive wastes [1].

One of the most important heavy metal is uranium because it contains chemical toxicity and radioactivity [1]. It has been classified as a confirmed human carcinogen by the EPA (The Environmental Protection Agency). The only acceptable limit for the risk of cancer from uranium is zero tolerance. Moreover, the maximum contaminant level (MCL) was accepted as 30 mg/L by the EPA (The Environmental Protection Agency). The interim maximum acceptable level (IMAC) was proposed as 20 mg/L by Canada, and the reference level was recommended as 2 mg/L by WHO [2, 3].

Some methods, for example adsorption, biosorption, ion exchange, and solvent extraction, have been developed to recover uranium from waste products [4–7]. Adsorption and ion exchange are among the most used methods for the

---

This work was supported by the Manisa Celal Bayar University (No. BAP 2012-005).

✉ Ümran Hiçsönmez
umran.hicsonmez@bayar.edu.tr

[1] Department of Primary School Science Teaching, Faculty of Education, Manisa Celal Bayar University, Manisa, Turkey

[2] Department of Chemistry, Faculty of Science and Art, Manisa Celal Bayar University, Manisa, Turkey

[3] Department of Physics, Faculty of Science and Art, Manisa Celal Bayar University, Manisa, Turkey

removal of uranium in industrial waste products. The clay and zeolite adsorbents known as natural adsorbent have sufficient sorption capacity. They are low cost, nontoxic, and abundant in nature. Further, the adsorption capacity of the clays is increased by expanding the clay pores and modifying various materials. In particular, the adsorption capacity of clays can be increased by using the calcinations technique, washing with acidic–alkali solutions, and affecting the inorganic cations [8–11].

The surface treatment of clay minerals with organic cations (usually quaternary ammonium compounds) can intensely modify the surface structures [12, 13]. A number of studies have used HDTMA (hexadecyltrimethylammonium)-modified clays and have shown their effectiveness in the removal of organic and metal ions such as phenol and Pb^{2+} ions from aqueous solutions [14–16]. Majdan et al. [17] examined the uranium adsorption on organo-bentonit treated with HDTMA and the structural properties of the adsorbent and adsorption products. Sprynskyy et al. [18] investigated the ability of natural and organic cation-modified diatomite (HDTMA–diatomite) to remove U(VI) ions. The maximum sorption capacities in the natural and the modified diatomite for U(VI) were found as 25.63 and 667.40 μmol/g, respectively.

Intensive magma and rock fragmentation are formed by volcanic eruptions. They produce volcanic ash. Volcanic ashes have particles with average diameters < 2 mm [19]. These volcanic ejecta, or tephras, contain various silicates and other minerals of different sizes such as volcanic glass, feldspar, quartz, hornblende, hypersthene, augite, magnetite, biotite, and apatite [20]. Kula basaltic volcanics were selected because they are abundant in nature, cheap, and an accessible sorbent. Kula is one of the areas in which the young volcanic rocks are seen in Turkey. The Kula volcanics are situated in an area with a length of 30–35 km and a width of 10–15 km in the Manisa province, Turkey. These are quaternary alkali basaltic lava flows and tephra. Tephra is a general term for fragments of volcanic rock and lava regardless of size, which are blasted into the air by explosions or carried upwards by hot gases in the eruption columns or porous structure lava fountains [21, 22]. In a study carried out by Kütahyalı et al. [22], the sorption of strontium ions on non-treated and HCl-treated with Kula volcanic was calculated as 2.04 and 1.72 mg/g, respectively.

In this study, the adsorption behavior of U(VI) on Kula basaltic organo-volcanics modified by (DEEA) was investigated. The parameters affecting the uranium adsorption in aqueous solutions, such as the concentration of organic cation, contact times, initial pH, uranium concentration, and temperature, were investigated, and the optimum conditions for the adsorption process were determined.

2 Materials and methods

2.1 Materials

The basaltic volcanics used in the present study were taken from the Manisa–Kula region of Turkey. Kula volcanics are classified as basic according to the rate of SiO_2 production, and basaltic according to their output temperature [23]. Kula basaltic volcanics were selected because they are abundant in nature, cheap, and an accessible sorbent.

A cationing surface-modifying agent (*N*,*N*-diethylethanolammonium chloride DEEA-Cl (C_6H_{13}-NO·HCl, WA 151.64 g/mol)), which is a quaternary ammonium salt, was used. A standard solution of 1000 mg/L U(VI) was prepared by dissolving a suitable amount of UO_2 $(CH_3COO)_2$ $2H_2O$ (Merck, Germany) in ultrapure water. The initial pH solutions were changed by HNO_3 or NaOH. U(VI) and the concentrations were determined by Arsenazo III [24]. A PG (UK) instrument T80 UV–Vis spectrophotometer was used. All reagents and solvents used were of an analytical grade.

2.2 Preparation of organo-volcanics

The organo-volcanics were prepared by treating the volcanics with an aqueous solution of DEEA) (Fig. 1). A total of 3 g of volcanics with 30 mL DEEA solution of different concentrations were added in flask, which was gently shaken for 24 h at 20 °C. Then, the DEEA-modified volcanics were centrifuged with 4000 rpm, washed five times with ultrapure water, and dried at 60 °C [8]. Thus, the volcanics were modified with the addition of DEEA amounts of 5, 10, 15, and 20 mM.

2.3 Characterization of organo-volcanics

The surface structure of the made organo-volcanic was examined under a FEI QUANTA 400F SEM scanning electron microscope at 1.2 nm resolution. The dried powders (approximately 0.01 g) were placed on a sticky carbon tape on standard Al mounts, then sputter coated with a thin conductive layer of gold. The chemical composition of the

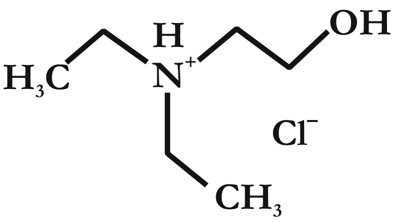

Fig. 1 *N*,*N*-Diethylethanolammonium chloride

basaltic original volcanic samples was analyzed by X-rays Fluorescence Spectroscopy (XRF), using a Spectro IQ II instrument. The interactions between DEEA and the volcanics were examined by FTIR spectroscopy. The FTIR spectra were obtained by using KBr pellets with a Perkin Elmer FTIR System/Spectrum BX. XRD patterns of the unmodified volcanics and the DEEA-uranium-modified volcanics were obtained by using X-ray diffraction analyses (PANALYTICAL Empyrean diffractometer), and the samples were scanned from 2 to 88 2-Theta in step sizes of 0.0130 and scanned at a step time of 148.92 s.

The surface areas of the volcanics were found by using the BET equation to the physical adsorption data for the nitrogen at 77 K. The unmodified and DEEA-volcanic samples were degassed in a vacuum at 573 and 323 K for 8 h, respectively. The (BET) analysis using the Autosorb 6 by Quantachrome Corporation was performed. The SEM–EDS images and BET were performed at the Central Laboratory of the Middle East Technical University in TURKEY.

2.4 Adsorption experiments

The uranyl acetate solution was added to the organo-volcanics. The sorption studies were carried out using the batch method. The mixture was shaken in a shaker (GFL 1083 model). The uranium(VI) percentage and adsorption uptake in the equilibrium, q_e (mg/g) were found by using the following equations:

$$\text{Removal efficiency } U\% = \frac{(C_o - C_e)}{C_o} \times 100, \tag{1}$$

$$q_e = (C_o - C_e) \times \frac{V}{m} \text{ (mg/g)}, \tag{2}$$

Where, C_o, is the initial concentration of U(VI) in the solution, (mg/L); C_e the equilibrium concentration of the uranium in the solution, (mg/L); V is the solution volume (L), and m is the dry adsorbent mass (g). The distribution coefficient, K_d (mL/g), was calculated using Eq. (3):

$$K_d = \frac{(C_o - C_e)}{C_e} \times \frac{V}{m}. \tag{3}$$

3 Results and discussion

3.1 Characteristic analysis

The chemical composition of the original basaltic volcanic sample was found to be composed of SiO_2, Al_2O_3, Fe_2O_3, MnO, MgO, CaO, Na_2O, K_2O, TiO_2, P_2O_5, and other trace elements at the percentages of 48.4; 17.66; 8.648; 0.085; 8.538; 6.234; 3.989; 2.881; 1.85, 0.625, and 1.09%, respectively. The morphologies, as well as the structural ordering of the natural and modified volcanic, are presented in Fig. 2a, b, respectively.

There are many crystals in the cavities of unmodified volcanics (Fig. 2a). It was observed that the morphology of the surface was changed by the DEEA surfactant (Fig. 2b). The volcanic surface was covered with the DEEA organic. The specific surface areas of the unmodified and DEEA-modified volcanics were found as 2.265 and 3.689 m^2/g by the multipoint BET method, respectively.

The FTIR spectra of DEEA organo-volcanic and U(VI)-DEEA organo-volcanic are shown in Fig. 3. For the DEEA organo-volcanic, the broad band around 3385 cm^{-1} in the DEEA organo-volcanic was attributed to the O–H stretching vibrations. Generally, the C–H stretching bands of the alkylammonium cations are found in the 3020–2800 cm^{-1} area [25]. For the modified volcanic, two weak bands were noted at 2945 and 2845 cm^{-1}. The HOH deformation peak at 1654 cm^{-1} was present in the FTIR spectrum of the DEEA organo-volcanic. Generally, the adsorbed was water contributing to the bending region in the 1600–1700 cm^{-1} area [24]. The strong band around 1031 cm^{-1} was ascribed to the Si–O stretching vibration. The stretching and bending vibrations of the SiO_4^{2-} tetrahedral were the peaks at 537 and 471 cm^{-1}. The absorption band at 695 cm^{-1} was attached to the coupled Al–O and Si–O out of plane vibrations [26].

In the case of the U(VI)-DEEA organo-volcanic, peaks similar to that of the organo-volcanic structure were detected in the region of 3200–3600 cm^{-1} where it is indicated Si–0, N–H, and O–H stretching vibrations. It was observed that the H–O-H deformation peak shifted from 1654 to 1641 cm^{-1} with adsorption. The changes in the absorption band related to the H–O–H deformation of water molecules adsorbed on the volcanic were shown by this band. The characteristic absorption peak of Si–O of the organo-volcanic was observed at 1031 cm^{-1}, and the Si–O of the uranium adsorption was expanded to the same range, which showed that the uranium is adsorbed on the volcanic surface. In addition, the peak at 695 cm^{-1} was shifted to the 654 cm^{-1} region.

According to the XRD patterns of natural volcanics, such minerals as quartz (SiO_2), coesite (SiO_2), potassium sodium aluminosilicate ($K_{0.667}$ $Na_{0.333}$) ($AlSiO_4$), magnesium iron aluminosilicate ($Mg_{0.34}$ $Fe_{1.66}$ Al_4), sekaninaite (Si_5O_{18}), calcium magnesium catena-silicate diopside high (Ca Mg Si_2O_6), and ferropargasite ($NaCa_2Fe_4Al(Si_6$ $Al_2)$ O_{22} $(OH)_2$ were determined in the samples. The XRD patterns of the unmodified volcanics and the DEEA-uranium-modified volcanics are shown in Fig. 4. The unmodified volcanics sample mostly consisted of the SiO_2 amorphous phases (Fig. 4). The X-ray pattern of the unmodified volcanics was different to the pattern of the treated one. Few new peaks of the organic cation are seen

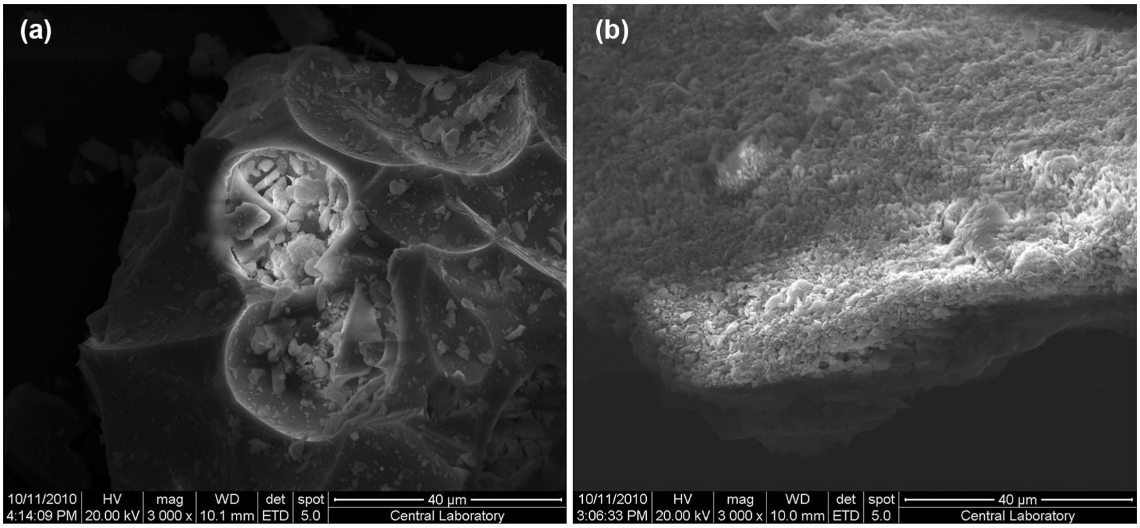

Fig. 2 SEM pictures of the Kula volcanics (**a**) and DEEA modified of Kula volcanics (**b**)

Fig. 3 FTIR spectra of organo-volcanic and U(VI) adsorbed to organo-volcanic

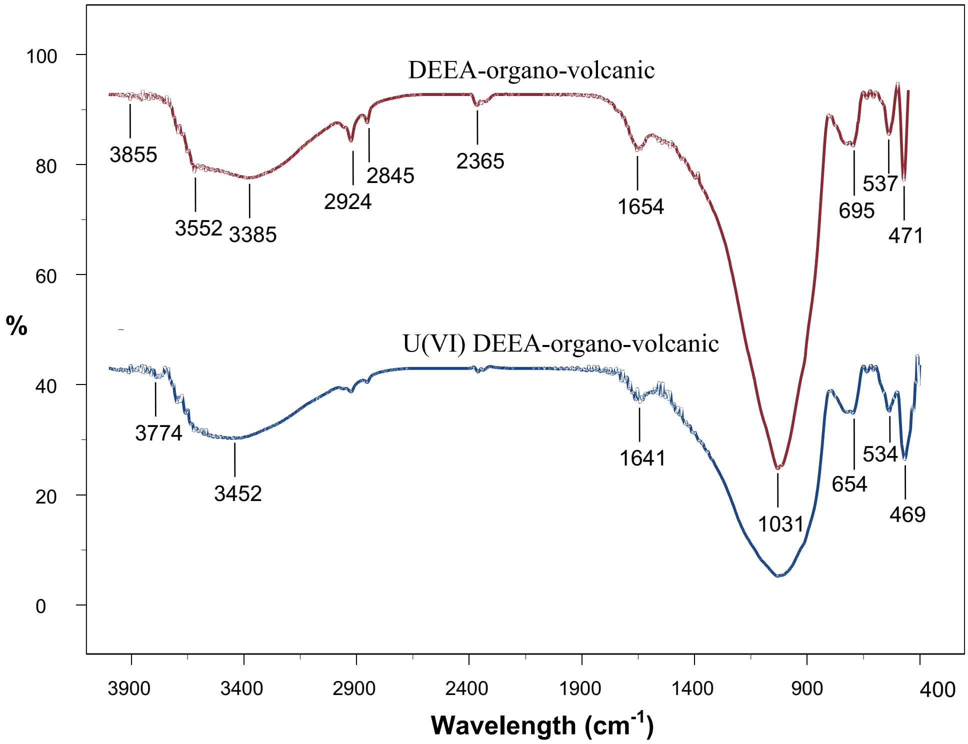

on the X-ray pattern of the DEEA-uranium modified material. They could originate from the DEEA cations and uranium deposited on the volcanics surface. Also, the uranium peak appeared on the pattern 34, 39 2-θ°. The uranium peaks are similar to those in literature [27, 28].

The surface area was calculated by using the multipoint BET method. The BET surface areas of unmodified volcanics and DEEA-modified volcanics were found as 2.265 and 3.689 m^2/g, respectively.

The zeta potentials of the unmodified and modified volcanics were measured in the pH range of 3–8. The surfaces of both the volcanics were found to be negatively charged. We believe that there was an electrostatic attraction on the volcanic surface between the negative charge of the SiO and AlO groups and the positive charge of the organic chain. However, the volcanic surface was also negatively charged because the DEEA concentration was low. In the literature, it has been emphasized that cationic surfactants covered all the clay surfaces and displacing

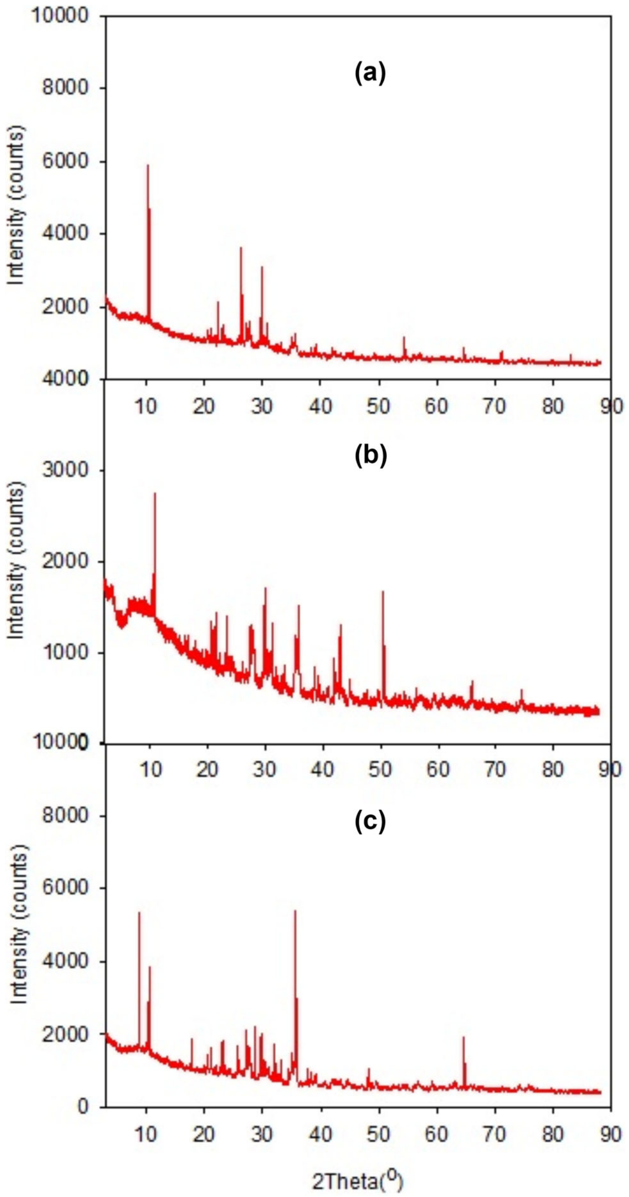

Fig. 4 X-ray diffraction patterns. **a** the unmodified, **b** the DEEA-modified and **c** DEEAU(VI) modified with volcanics

expanded by entering of the organic molecules between the sheet layers of the clay minerals [29].

3.2 Batch adsorption experiment

3.2.1 Effect of different concentrations of organic cation

The effect of the organic cation concentration (5, 10, 15, and 20 mM) on the adsorption was examined in a media solution of 20 mg/L U(VI). The maximum U(VI) adsorption was found at 5 mM DEEA. When the organic cation concentration reached 5 mM micelle formation, it became more efficient than the interaction of the hydrocarbon chains. After this critical micelle point, the absorption capacity decreases [25].

3.2.2 Effect of contact time

The time dependence of the U(VI) adsorption experiments is given in Fig. 5 under the conditions of 1 g adsorbent, a volume of 30 mL, 20 mg/L U(VI), pH of 3.5, and a temperature of 25 °C. The sorption of the U(VI) was increased from 61.15 to 76.30% after 4 h. Equilibrium was reached within 4 h.

3.2.3 Effect of initial pH values

The effect of the initial pH on the U(VI) sorption was examined by adjusting it to different values ranging from 2.0 to 6.0 (30 mL solution and 20 mg/L U(VI)). The solution and volcanics were mixed at 25 °C for 4 h. The U (VI) sorption strongly depended on the pH solution and increased with the increasing pH (Fig. 6) [24].

At a low pH (below pH 4), when the dissociation of the Si–OH bonds is suppressed, the adsorption of the U(VI) is low. The UO_2^{2+} in the acidic solutions is the only complex-forming uranium species ($(UO_2)_2CO_3(OH)_3^-$, UO_2-OH^+, $UO_2(OH)_2$, $(UO_2)_2(OH)_2^{2+}$, $(UO_2)_3(OH)_5^+$, and UO_2CO_3, etc.) [14]. $(UO_2)_2(OH)_2^{2+}$) and $(UO_2{\cdot}OH)^+$ hydrolysis species were found between pH 3.0 and 4.0. also, the $(UO_2)_3(OH)_5^+$ forms at pH 4.0 and becomes dominant at the pH values exceeding 4.5 [30]. In this study, the optimum pH was found as 5.0.

3.2.4 Effect of initial U(VI) concentration

The effect of the initial concentration of U(VI) was examined by contacting a mass of DEEA organo-volcanics (1 g) at 25 °C and an initial pH = 5.0 using a range of U (VI) concentrations (20, 40, 60, 80, and 100 mg/L) (Fig. 7). The removal of the U(VI) was increased by increasing the initial U(VI) concentration between 20 and 40 mg/L. Moreover, the adsorption capacity of the DEEA-volcanics for U(VI) was decreased by increasing the initial uranium concentration (after 40 mg/L). The optimum concentration was found to be 40 mg/L.

3.2.5 Adsorption isotherms

Adsorption isotherms show the equilibrium relationships between the adsorbed ion concentrations and ion concentrations in a solution. In our work, the Langmuir, Freundlich and Dubinin–Radushkevich isotherm adsorption models, the most commonly used models, were also employed to describe the sorption behaviors. The Langmuir isotherm model assumes that the sorption occurs on a

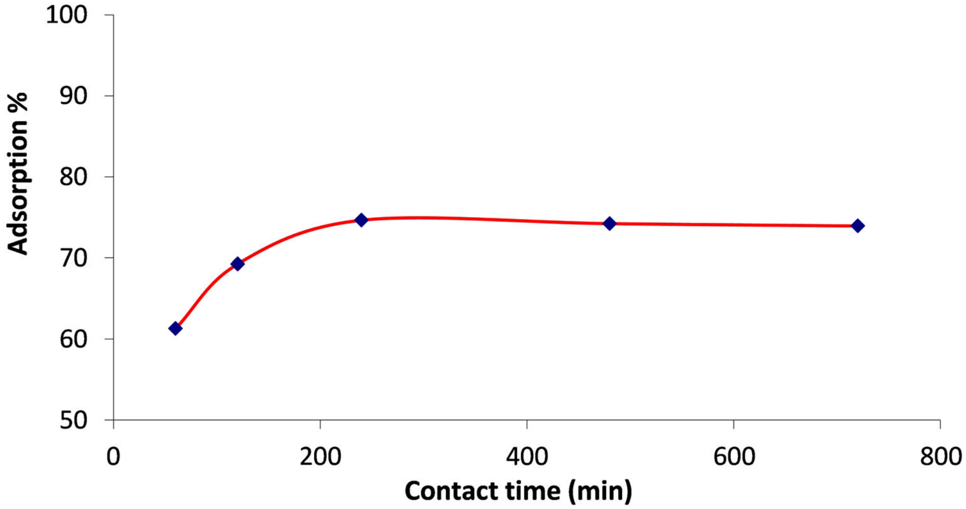

Fig. 5 Effect of contact time on removal of U(VI)

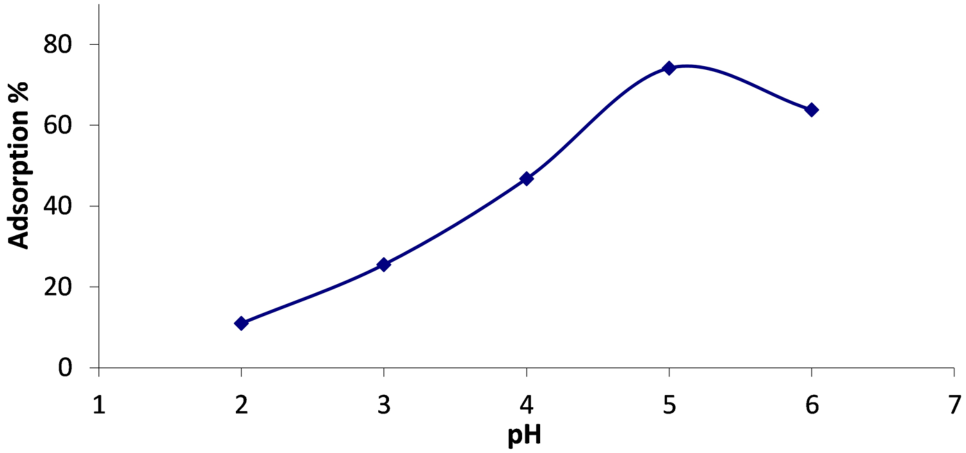

Fig. 6 Effect of pH on removal of U(VI)

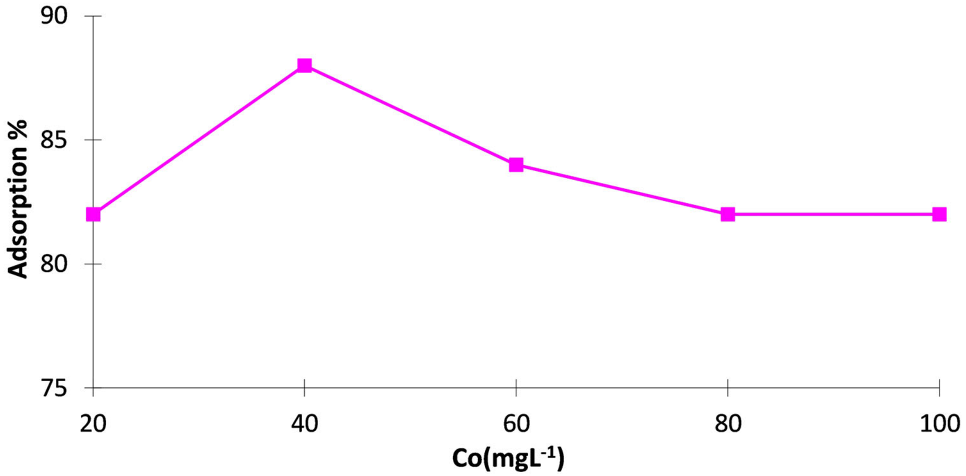

Fig. 7 Effect of initial U(VI) concentration on removal U(VI)

homogeneous surface by the monolayer sorption. The Langmuir adsorption isotherm model is represented as Eq. (4),

$$\frac{C_e}{q_e} = \frac{1}{K_L q_m} + \frac{C_e}{q_m}, \tag{4}$$

Where q_m (mg/g) is the maximum amount of adsorption of U(VI) per unit mass of the adsorbent, and K_L (L/mg) is the Langmuir affinity constant that represents the affinity between the adsorbent and the adsorbate.

Freundlich isotherm, the linear equation is expressed by Eq. (5),

$$\log q_{\mathrm{e}} = \log K_{\mathrm{F}} + \frac{1}{n}\log C_{\mathrm{e}}, \tag{5}$$

where K_{F} [(mg/g)(L/mg)$^{1/n}$] is the constant related to the adsorption capacity of the adsorbent, $1/n$ is the constant related to the adsorption intensity of the adsorbent. The Freundlich isotherms were based on the adsorption on the heterogeneous solid surfaces.

Dubinin–Radushkevich isotherm is generally applied to express the adsorption mechanism with a Gaussian energy distribution onto a heterogeneous surface. The model has often successfully fitted high solute activities and the intermediate range of concentrations data well.

$$\ln q_{\mathrm{e}} = \ln(q_{\mathrm{s}}) - (K_{\mathrm{ad}}\varepsilon^2), \tag{6}$$

Where q_{e}, q_{s}, K_{ad}, ε are q_{e}: amount of adsorbate in the adsorbent at equilibrium (mg/g); q_{s} is the theoretical isotherm saturation capacity (mg/g); K_{ad}: Dubinin–Radushkevich isotherm and is constant (mol^2/kJ^2) and ε: Dubinin–Radushkevich isotherm and is constant. The approach is usually applied to distinguish the physical and chemical adsorption of metal ions with its mean free energy. The E per molecule of the adsorbate (for removing a molecule from its location in the sorption space to the infinity) can be computed by the relationship (7):

$$E = \left[\frac{1}{\sqrt{2B_{\mathrm{DR}}}}\right], \tag{7}$$

Where B_{DR} is denoted as the isotherm constant. Meanwhile, the parameter, ε, can be calculated by Eq. (8):

$$\varepsilon = RT\ln\left[1 + \frac{1}{C_{\mathrm{e}}}\right], \tag{8}$$

Where R, T, and C_{e} represent the gas constant (8.314 J/mol K), the absolute temperature (K), and adsorbate equilibrium concentration (mg/L), respectively.

We also tested the Langmuir, Freundlich, and D–R adsorption isotherms, and the results indicated that the D–R adsorption isotherm ($R^2 > 0.96$) fitted the data better than the Langmuir and Freundlich adsorption isotherms. All the results are listed in Table 1.

From this research work, the maximum monolayer coverage capacity (q_{m}) from the Langmuir Isotherm model was determined to be 400 mg/g, K_{L} (Langmuir isotherm constant) is 0.014 L/mg, and the R^2 value is 0.31.

The Freundlich isotherm constants k_{f}, and n were determined from the intercept and slope of a plot of log q_{e} versus log C_{e} (Fig. 8).

From the data in Table 1, it can be seen that value of 1/ n is 0.9061, the sorption of U(VI) on to DEEA organo-volcanics is favorable and the R^2 value is 0.9564. Thus, the adsorption process is multilayered.

In addition, from the linear plot of the D–R model, q_{s} was determined to be 74.24 mg/g, the mean free energy, E was 11.18 kJ/mol indicating a chemical adsorption process, and the R^2 was 0.9646 higher than that of the Freundlich.

Essentially, the DEEA organo-volcanic shows very good sorption performance for U(VI) in comparison with other adsorbents reported in the literature in Table 2.

Uranium adsorption onto DEEA organo-volcanics is shown schematically in Fig. 9.

3.2.6 *Adsorption kinetics*

The kinetics of adsorption is an important aspect in defining the efficiency of the adsorption process. The kinetic data in this study were modeled using pseudo-first-order [36] and pseudo-second-order [2] according to:

$$\text{Pseudo-first-order} \quad \ln q_{\mathrm{t}} = \ln q_{\mathrm{e}} - k_1 t, \tag{9}$$

$$\text{Pseudo-second-order} \quad q_{\mathrm{t}} = \frac{1}{k_2 q_{\mathrm{e}}^2} + \frac{1}{q_{\mathrm{e}} t}, \tag{10}$$

Where q_{e} and q_t are the adsorption capacity (mg/g) at equilibrium and time ‘t,’ respectively, k_1 and k_2 are the pseudo-first-order and pseudo-second-order constants of the adsorption, respectively. The relationships of $\ln(q_t - q_{\mathrm{e}})$ to t t/q_t to t were plotted according to the experimental values (Fig. 10).

The adsorption kinetic data were ideally described by the pseudo-second-order equation ($R^2 = 0.9999$). q_{e} and k_2 were obtained and represented in Table 3.

3.2.7 *Thermodynamics studies*

Entropy ($\Delta S°$) and Gibbs free energy ($\Delta G°$) factors were used to determine the processes occurring spontaneously. The thermodynamic data can be calculated with the

Table 1 Equilibrium isotherm parameters of sorption of U(VI) by DEEA organo-volcanics

Langmuir			Freundlich			D–R			
q_{m} (mg/g)	K_{L} (L/mg)	R^2	K_{F} (mg/g)	$1/n$	R^2	q_{s} (mg/g)	K_{ad} (mol^2/kJ^2)	E (KJ/mol)	R^2
400	0.0144	0.3131	2.2	0.9061	0.9564	74.24	0.0040	11,18	0.9646

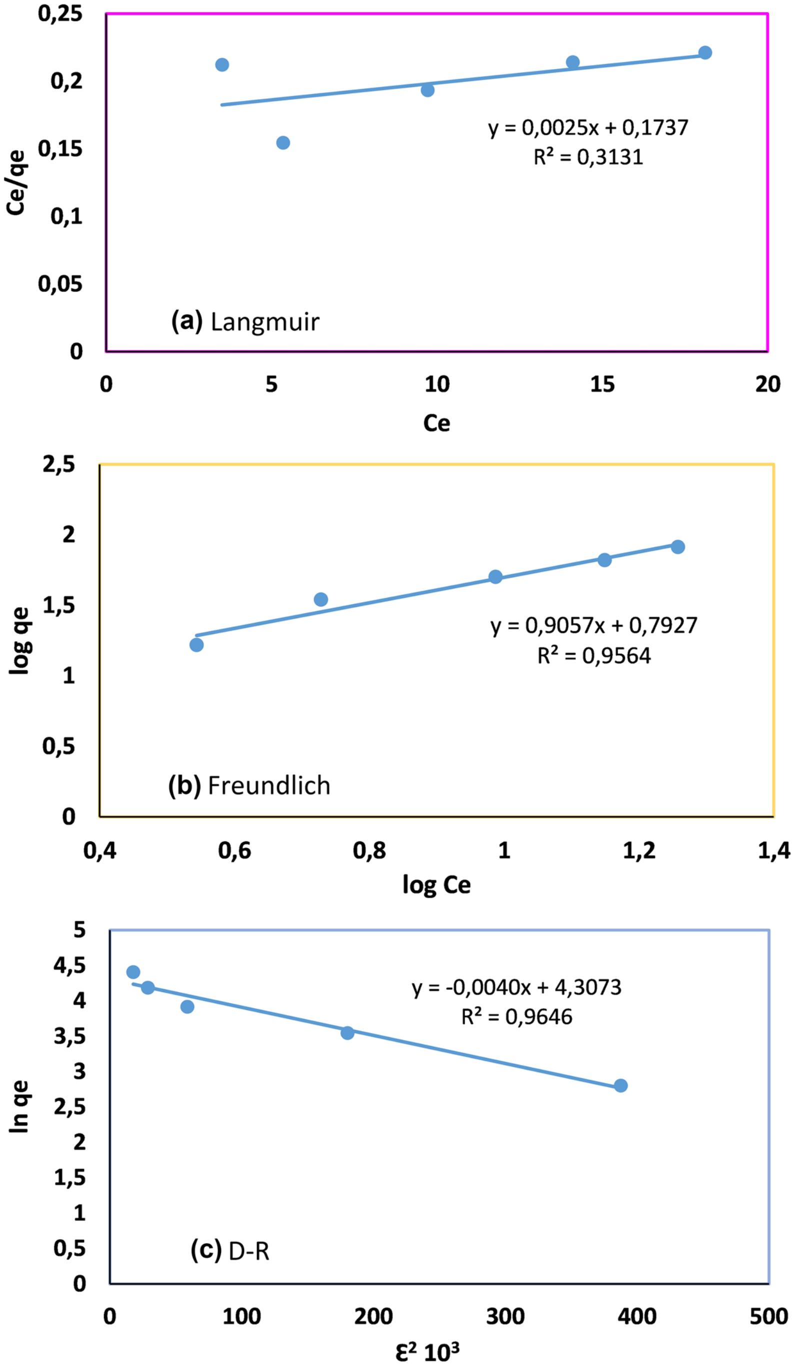

Fig. 8 The linearized isotherms for adsorption of U(VI) by DEEA organo-volcanics

thermodynamic distribution coefficient (K_d). $\Delta G°$, $\Delta H°$ (enthalpy change), and the $\Delta S°$ were calculated with the Eq. 11 [37].

$$\ln K_d = \frac{\Delta S^{\circ}}{R} - \frac{\Delta H^{\circ}}{RT}, \qquad (11)$$

Where T the absolute temperature (K) and R the gas constant (kJ/molK). $\Delta G°$ value was calculated from (Eq. 12):

$$\Delta G^{\circ} = \Delta H^{\circ} - T\Delta S^{\circ} \qquad (12)$$

The experiments were done at different temperatures for a solution concentration of 40 mg/L of uranium. The values of $\Delta H°$ and $\Delta S°$ were calculated from the slopes and intercepts of the linear regression of $\ln K_d$ versus $1/T$. According to Table 4, the process is endothermic and the adsorbent adsorption capacity increases with increasing temperatures.

When the ions are adsorbed on the adsorbent surface, the water molecules that previously bonded onto the metal

Table 2 The comparison of the Freundlich adsorption capacities (K_F; mg/g) of different natural adsorbents toward U(VI) in the literature

Adsorbent	K_F (mg/g)	pH	References
Wood powder	0.461	8	[31]
Wheat straw	0.346	7	[31]
Hematite	1.63	7	[2]
Talc	2.19	5	[32]
Natural clinoptilolite zeolite	0.087	6	[33]
Goethite-coated sand	0.064	9	[34]
Polyacrylamidoxime resin-coated quartz sand	1.0	6	[35]
DEEA organo-volcanics	2.2	5	This Study

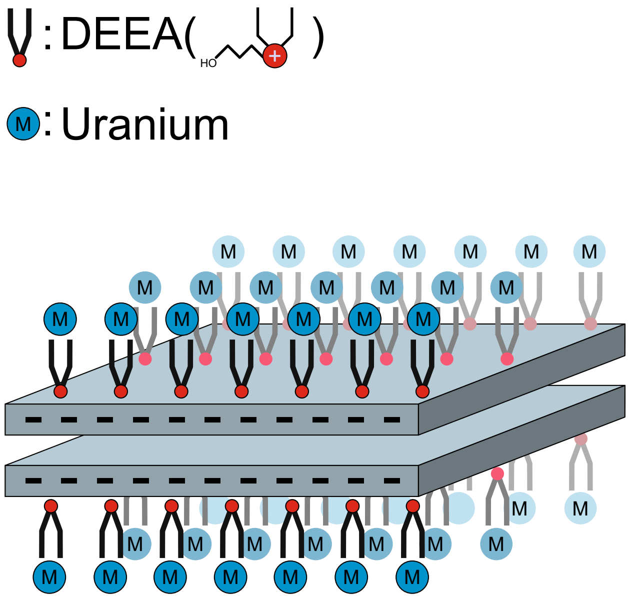

Fig. 9 Schematic illustration of the U(VI) adsorption on DEEA modified organo-volcanics

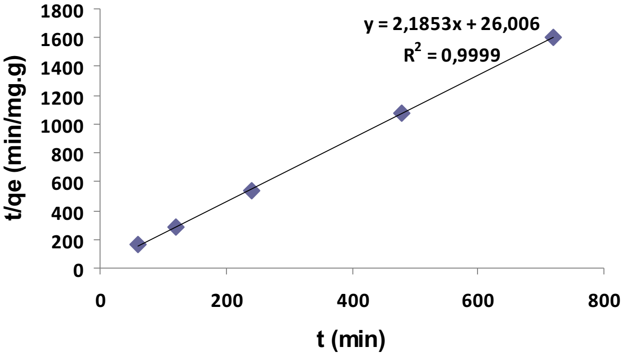

Fig. 10 Pseudo-second-order kinetic plots for the adsorption of U (VI) ions from aqueous solutions onto DEEA organo-volcanics

ion are released and dispersed into the solution. They lead to an increase in the entropy [38].

Table 3 The calculated parameters of the pseudo-second-order kinetic models

Temperature (K)	q_e (mg/g)	k_2 (g/mg min)	R^2
298	0.458	0.183	0.999

4 Conclusions

The removal of U(VI) on DEEA organo-volcanics was examined as the parameters (times, initial pH, temperature, and initial concentration of U(VI)). The uranium adsorption and K_d value of the natural volcanic after treatment with DEEA increased from 25% ± 0.76 to 88% ± 1.04 and from 10.08 to 220 mL g^{-1}, respectively. The studies on XRD and SEM analyses give characteristic results and indicated that DEEA penetrated into the clay interlayer. The data examined handling the adsorption models (Langmuir, Freundlich and D–R) in the equilibrium. The Freundlich and D–R isotherms on heterogeneous surfaces provided the best correlation with the uranium adsorption. The rate of the process can be represented very well by the pseudo-second-order kinetic model. The temperature reliance of the U(VI) adsorption on DEEA organo-volcanic was examined, and the thermodynamic data $\Delta H°$, $\Delta G°$ and $\Delta S°$ were analyzed. The sorption process was a physical adsorption process for enthalpy exchange in 2.2 kJ mol^{-1}. The result shows an endothermic heat of adsorption, but a negative free energy value, indicating that the process of uranium adsorption is favored at high temperatures. Because the volcanics are both cheap and abundant, DEEA organo-volcanic may be used as an efficient material for the U(VI) adsorption from aqua media. Kula volcanoes, which are found easily, made a natural adsorbent by increasing the capacity with ecologically harmless organic cations. Thus, these adsorbents will be useful in cleaning up nuclear waste containing radionuclides and in eradicating the problems and hazards in the environment.

Table 4 Thermodynamic parameters of U(VI) adsorption by DEEA organo-volcanics

$\Delta H°$	$\Delta S°$	$\Delta G°$ (KJ/mol)				
(KJ/mol)	(KJ/mol K)	293 K	303 K	313 K	323 K	333 K
2.2	0.05	− 13.49	− 14.02	− 14.56	− 15.09	− 15.63

Acknowledgements This work was supported by Manisa Celal Bayar University under Project BAP 2012-005. The authors would like to thank the Central Laboratory of the Middle East Technical University for the analysis of the SEM and BET values in the samples.

References

1. B. Benedict, T.H. Pigford, H.W. Levi, *Nuclear Chemical Engineering* (McGraw-Hill, New York, 1981), pp. 120–220
2. X. Shuibo, Z. Chun, Z. Xinghuo et al., Removal of uranium(VI) from aqueous solution by adsorption of hematite. J. Environ. Radioact. **100**, 162–166 (2009). https://doi.org/10.1016/j.jenvrad.2008.09.008
3. D. Zhao, X. Wang, S. Yang et al., Impact of water quality parameters on the sorption of U(VI) onto hematite. J. Environ. Radioact. **103**, 20–29 (2012). https://doi.org/10.1016/j.jenvrad.2011.08.010
4. K. Nazari, M.G. Maragheh, A.J. Rad, Studies on extraction of uranium from phosphoric acid using PN-1200 extractant. Hydrometallurgy **71**, 371–377 (2014). https://doi.org/10.1016/S0304-386X(03)00088-4
5. H.R. Shakur, R.E. Saraeea, M.R. Abdib et al., Highly selective and effective removal of uranium from contaminated drinking water using a novel PAN/AgX/ZnO nanocomposite. Microporous Mesoporous Mater. **234**, 257–266 (2016). https://doi.org/10.1016/j.micromeso.2016.07.034
6. H.R. Shakur, R.E. Saraeea, M.R. Abdib et al., Selective removal of uranium ions from contaminated waters using modified-X nanozeolite. Appl. Radiat. Isot. **118**, 43–55 (2016). https://doi.org/10.1016/j.apradiso.2016.08.022
7. U.H. Kaynar, M. Ayvacıklı, S.C. Kaynar et al., Removal of uranium(VI) from aqueous solutions on nanoporous ZnO by manufactured microwave-assisted combustion synthesis. J. Radioanal. Nucl. Chem. **299**, 1469–1477 (2014). https://doi.org/10.1007/s10967-014-2919-2
8. A.M. Yusof, N.A.N.N. Malek, Removal of Cr(VI) and As (V) from aqueous solutions by HDTMA-modified zeolite Y. J. Hazard. Mater. **162**, 1019–1024 (2008). https://doi.org/10.1016/j.jhazmat.2008.05.134
9. U. Wingenfelder, G. Furrer, R. Schulin, Sorption of antimonate by HDTMA-modified zeolite. Microporous Mesoporous Mater. **95**, 265–271 (2006). https://doi.org/10.1016/j.micromeso.2006.06.001
10. S.Y. Lee, S.J. Kim, Adsorption of naphthalene by HDTMA modified kaolinite and halloysite. Appl. Clay Sci. **22**, 55–63 (2002). https://doi.org/10.1016/S0169-1317(02)00113-8
11. M. Borisover, Z. Gerstl, F. Burshtein et al., Organic sorbate-organoclay interactions in aqueous and hydrophobic environments: sorbate-water competition. Environ. Sci. Technol. **42**, 7201–7206 (2008). https://doi.org/10.1021/es801116b
12. Y. Xi, R. Frost, H. He, Modification of the surfaces of Wyoming montmorillonite by the cationic surfactants alkyl trimethyl, dialkyl dimethyl, and trialkyl methyl ammonium bromides. J. Colloid Interface Sci. **305**, 150–158 (2007). https://doi.org/10.1016/j.jcis.2006.09.033
13. C.H. Ryu, S.D. Yeo, Vapor phase adsorption of trichloroethane using organically modified montmorillonite. J. Indian Eng. Chem. **377**, 441–449 (2010). https://doi.org/10.1016/j.jiec.2010.01.043
14. S. Richards, A. Bouazza, Phenol adsorption in organo-modified basaltic clay and bentonite. Appl. Clay Sci. **37**, 133–142 (2007). https://doi.org/10.1016/j.clay.2006.11.006
15. J.Q. Jiang, C. Cooper, S. Ouki, Comparison of modified montmorillonite adsorbents: part I: preparation, characterization and phenol adsorption. Chemosphere **47**, 711–716 (2002). https://doi.org/10.1016/S0045-6535(02)00011-5
16. J.J. Lee, J. Choi, J.W. Park, Simultaneous sorption of lead and chlorobenzene by organobentonite. Chemosphere **49**, 1309–1315 (2002). https://doi.org/10.1016/s0045-6535(02)00531-3
17. M. Majdan, S. Pikus, A. Gajowiak et al., Characterization of uranium(VI) sorption by organobentonite. Appl. Surf. Sci. **256**, 5416–5421 (2010). https://doi.org/10.1016/j.apsusc.2009.12.123
18. M. Sprynskyy, I. Kovalchuk, B. Buszewski, The separation of uranium ions by natural and modified diatomite from aqueous solution. J. Hazard. Mater. **181**, 700–707 (2010). https://doi.org/10.1016/j.jhazmat.2010.05.069
19. B. Zimanowski, K. Wohletz, P. Dellino et al., The volcanic ash problem. J. Volcanol. Geotherm. Res. **122**, 1–5 (2003). https://doi.org/10.1016/S0377-0273(02)00471-7
20. M. Nanzyo, Unique properties of volcanic ash soils. Glob. Environ. Res. **6**, 99–112 (2002)
21. T. Ercan, Interpretation of geochemical, radiometric and isotopic data on Kula volcanics (Manisa-W. Anatolia). Geol. Bull. Turkey **36**, 113–129 (1993)
22. C. Kütahyalı, B. Cetinkaya, M.B. Acar et al., Investigation of strontium sorption ont Kula volcanic using central composite design. J. Hazard. Mater. **201–202**, 115–124 (2012). https://doi.org/10.1016/j.jhazmat.2011.11.047
23. R.V. Fisher, Proposed classification of volcaniclastic sediments and rocks. Geol. Soc. Am. Bull. **72**, 1409–1414 (1961). https://doi.org/10.1130/0016-7606(1961)72%5B1409:PCOVSA%5D2.0.CO;2
24. G. Wang, X. Wang, X. Chai et al., Adsorption of uranium(VI) from aqueous solution on calcined and acid-activated kaolin. Appl. Clay Sci. **47**, 448–451 (2010). https://doi.org/10.1016/j.clay.2009.11.003
25. J. Madejova, FTIR techniques in clay mineral studies. Vib. Spectrosc. **31**, 1–10 (2003). https://doi.org/10.1016/S0924-2031(02)00065-6
26. T.S. Anirudhan, C.D. Bringle, S. Rijith, Removal of uranium(VI) from aqueous solutions and nuclear industry effluents using humic acid-immobilized zirconium-pillared clay. J. Environ. Radioact. **101**, 267–276 (2010). https://doi.org/10.1016/j.jenvrad.2009.12.001
27. H. Einspahr, J.R. Donohue, Golden book of phase transitions. Wroclaw **1**, 1–123 (2002)
28. P.E. Tomaszewski, Structural phase transitions in crystals. I. Database. Phase Transit. **38**, 127–220 (1992). https://doi.org/10.1080/01411599208222899
29. Y. Xi, R.L. Frost, H. He et al., Modification of wyoming montmorillonite surfaces using a cationic surfactant. Langmuir **21**, 8675–8680 (2005). https://doi.org/10.1021/la051454i
30. C. Kütahyalı, M. Eral, Selective adsorption of uranium from aqueous solutions using activated carbon prepared from charcoal

by chemical activation (G-7). Sep. Purif. Technol. **40**, 109–114 (2004). https://doi.org/10.1016/j.seppur.2004.01.011

31. S. Bagherifam, A. Lakzian, S.J. Ahmadi et al., Uranium removal from aqueous solutions by wood powder and wheat straw. J. Radioanal. Nucl. Chem. **283**, 289–296 (2010). https://doi.org/10.1007/s10967-009-0348-4
32. M. Sprynskyy, T. Kowalkowski, H. Tutu et al., Adsorption performance of talc for uranium removal from aqueous solution. Chem. Eng. J. **171**, 1185–1193 (2011). https://doi.org/10.1016/j.cej.2011.05.022
33. L.M. Camacho, S. Deng, R.R. Parra, Uranium removal from groundwater by natural clinoptilolite zeolite: effects of pH and initial feed concentration. J. Hazard. Mater. **175**, 393–398 (2010). https://doi.org/10.1016/j.jhazmat.2009.10.017
34. U. Gabriel, J.P. Gaudet, L. Spadini et al., Reactive transport of uranyl in a goethite column: an experimental and modelling study. Chem. Geol. **151**, 107–128 (1998). https://doi.org/10.1016/s0009-2541(98)00074-6
35. S.C. Barton, D.I. Stewart, K. Morrisb et al., Performance of three resin-based materials for treating uranium-contaminated groundwater within a PRB. J. Hazard. Mater. **116**, 191–204 (2004). https://doi.org/10.1016/j.jhazmat.2004.08.028
36. S. Lagergren, B.K. Sven, Vatenskapasad. Handl. **24**, 1–36 (1898)
37. H.K. Boparai, M. Joseph, D.M. O'Carroll, Kinetics and thermodynamics of cadmium removal by adsorption onto nano zerovalent iron particles. J. Hazard. Mater. **186**, 458–465 (2011). https://doi.org/10.1016/j.jhazmat.2010.11.029
38. A. Rahmati, A. Ghaemi, M. Samadfam, Kinetic and thermodynamic studies of uranium(VI) adsorption using Amberlite IRA-910 resin. Ann. Nucl. Energy **39**, 42–48 (2012). https://doi.org/10.1016/j.anucene.2011.09.006